Geologie en Mijnbouw **76:** 321–338, 1998.

Diapirism synchronous with regional deformation and gold mineralisation, a new concept for granitoid emplacement in the Southern Cross Province, Western Australia

H.J. Dalstra, E.J.M. Bloem, J.R. Ridley & D.I. Groves
Key Centre for Strategic Mineral Deposits, Department of Geology and Geophysics, The University of Western Australia, Nedlands, WA, 6009, Australia

Received 13 April 1994; accepted in revised form 10 October 1997

Key words: Archean, greenstone belts, tectonic concepts

Abstract

The Southern Cross Province in the Archean Yilgarn Block of Western Australia comprises large dome-shaped granitoid bodies surrounded by narrow greenstone belts. Determination of the emplacement mechanism of these domes is fundamental for understanding the tectonic history of this region. Many structures in the greenstone belts show trends which reflect their tectonic relationships with the granitoid domes. Some of these structures host large gold occurrences. The domes have concentric foliation patterns, both within the granitoids themselves, and in the neighbouring greenstone belts. The smaller domes only have radial mineral lineation patterns in their wall rocks, but the largest dome, the Ghooli Dome, has also a tangential pattern. The prevailing gentle dip of the foliation in the centre of this dome and the abundance of greenstone xenoliths suggest that the present exposures are close to its roof. Geothermometry and geobarometry on mineral assemblages in the Ghooli granitoid and its xenoliths show that its crystallisation temperature was just above 700 °C at a relatively high pressure of 4.3 to 6.2 kbar. These P-T conditions are higher than those inferred for peak metamorphism in the greenstones. Therefore, this granitoid must have been emplaced initially at crustal levels deeper than the maximum burial of the greenstones which flank the dome. The Ghooli Dome has a SHRIMP U-Pb zircon age of 2691 ± 7 Ma. Diapiric rise of the granitoid plutons taking place in a regional compressive tectonic regime is considered to be the most likely mechanism for the final emplacement of these bodies into their host rock at about 2636–2620 Ma. This concept is preferred over the alternatives because it best reconciles the calculated P-T data, the observed structural patterns, the presence of pegmatites and aplites in the host rock, and the orientation of the mineral-bearing structures.

Introduction

Archean granitoid–greenstone terrains are an important component of Archean cratons worldwide. In general, these terrains are granitoid-dominated, with relatively shallow greenstone belts sited within widespread heterogeneous gneisses, tonalites, granodiorites, quartz-monzonites and granites (Archibald et al. 1981). Rocks of granitic, granodioritic and tonalitic composition, hereafter referred to as granitoids, make up approximately 75% of the outcrop in the Southern Cross Province of the Yilgarn Block, Western Australia. In the only detailed study on granitoids in this province, Bettenay (1977) subdivided the granitic rocks on the basis of their structural characteristics into pre-kinematic gneisses, syn-kinematic granitoids and post-kinematic granitoids with fractionated leucoadamellites. For their emplacement, he preferred a model which involved basement reactivation leading to granitoid plutonism and metamorphism, in response to elevated temperature conditions above mantle disturbances.

The most recent regional study carried out on granitoids in the Yilgarn Block, largely in the Eastern Goldfields Province, by Hill et al. (1992), showed that two major felsic episodes occurred in the block. An early episode of granodiorite, monzogranite and tonalite emplacement took place at 2690–2685 Ma and was

followed by a second episode of monzogranite, diorite and granodiorite emplacement at 2665–2660 Ma. Later, the by then highly fractionated felsic intrusions intruded the sequences until 2600 Ma.

Traditionally, granitoids of the Yilgarn Block are not regarded as metallogenetically significant. However, recent studies on the origin of the fluids which caused the lode-gold mineralisation, invoke giant plumbing systems and deep sources of these fluids, well below the maximum burial depth of the greenstone belts. They point either to equilibration of lower crustal or mantle-derived fluids with older granitic crust, or to exsolution of the fluids from a granitic magma derived from such a crust (Groves 1993).

The compositions of granitoids in the area around Southern Cross (Figure 1) are plotted in a $CaO–K_2O–Na_2O$ triangular plot (Figure 2) using selected data of Bettenay (1977). The granitoids form a tightly clustered group with a clear compositional trend towards K-enrichment which is strongest in garnet–muscovite granites.

In the Southern Cross Province, there is a spatial and structural relationship between large gold occurrences and specific Archean granitoid domes, which justifies a structural study of these domes and their country rocks (Figure 1). In this paper, the petrological and geochemical aspects of the granitoids east of Southern Cross are briefly discussed, followed by a discussion of their structural characteristics, timing and relationship to the regional greenstone-belt deformation and metamorphism. The four main objectives of this paper are:

1) to describe the large-scale structural patterns within the granitoid domes and country rocks;
2) to determine the depth of emplacement of the granitoids, and to compare this with the maximum burial depth of the country rocks;
3) to determine the timing of crystallisation of the largest granitoid mass in the region, the Ghooli granitoid;
4) to introduce a tectonic concept which best explains the structural and metamorphic patterns and to briefly discuss the implications for gold mineralisation. A future paper will deal in more detail with the gold mineralisation in relation to regional deformation and granitoid emplacement.

The plutons and their host rocks

The granitoids

Granitic rocks in the Southern Cross region display an array of features characteristic for structural processes under high P and T conditions which range from gneissic banding to syntectonic and posttectonic granitoid emplacement (Bettenay 1977). They also have a minor component of garnet–muscovite granite similar to those described for the Abitibi terrain in Canada by Feng and Kerrich (1992).

Three major domes of tonalitic to monzogranitic composition were distinguished in the terrain east of Southern Cross on the basis of field mapping, structural analysis of aerial photographs and aeromagnetic data (Figure 1). As there are no cross-cutting relationships between these domes, their emplacement was probably broadly contemporaneous. The domes are cut to the east by the Koolyanobbing Shear Zone. A sinistral, strike-slip shear component on this zone is inferred from subhorizontal mineral lineations and pressure shadows on feldspar clasts, and is also suggested by sinistral offset of regional aeromagnetic trends over several kilometres in the granitoid terrain (Libby et al. 1991).

The northern *Hamersley Dome* is a N–S elongated, ovoid body, approximately 40 km long and 20 km wide, characterised by a concentric magmatic foliation pattern and subvertical mineral lineations which plunge in a radial pattern in the adjacent greenstone belt to the west (Figures 3A, B). The foliation in the central part of the dome is formed by elongate feldspar and magmatic biotite and muscovite crystals. Parallel to the foliation are thin aplitic and pegmatitic veins which are boudinaged. On the margin of the dome, a strong recrystallised fabric in the granitoid and a secondary shear-band cleavage (S-C fabric) are present. Their geometry suggests a dome-up movement. A preferred orientation of quartz crystals defines a steep, down-dip mineral lineation in the granitoid. In the granitoid–greenstone contact zones there are frequent xenoliths of greenstone which are metamorphosed to amphibolites. These xenoliths have strong hornblende–plagioclase foliations which are always parallel to the foliation in the adjacent granitoid. The greenstone adjacent to the granitoid is frequently intruded by pegmatite dikes which have a foliation parallel to that in the adjacent granitoid and greenstones. Massive quartz veins, which are up to 10 m thick and hundreds of metres long, run parallel to the granitoid–greenstone contact. Locally

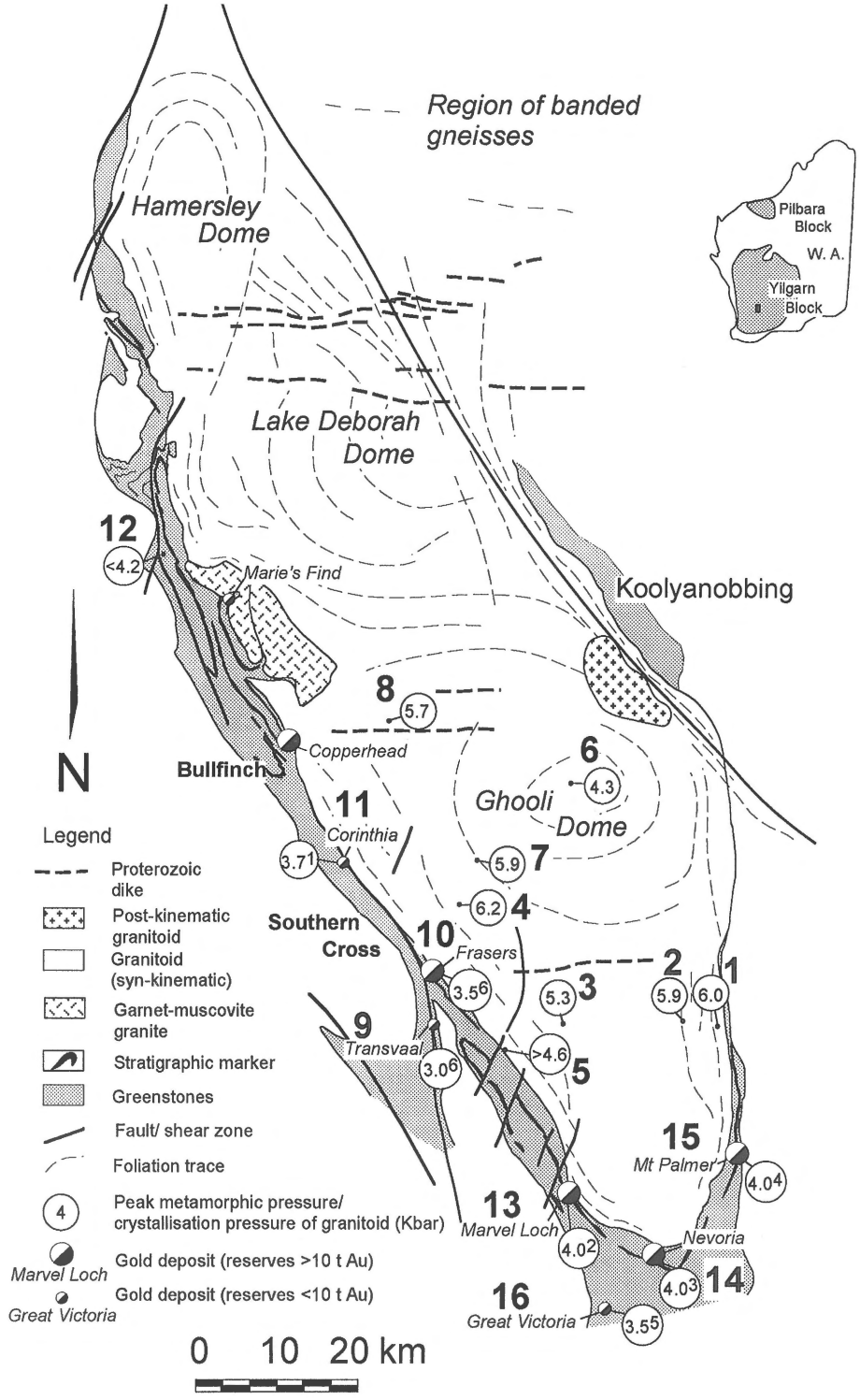

Figure 1. Interpretative map of the Ghooli Dome complex and the surrounding greenstone belts. Locations 1–16 represent areas for which peak-metamorphic conditions or P-T calculations of crystallisation are presented in Table 1. Additional P-T estimates are from:[1] Bloem et al. (1994), [2] and [3] Mueller (1990), [4] Gole and Klein (1981), [5] McQueen (1992), and [6] Dalstra and Ridley (1993).

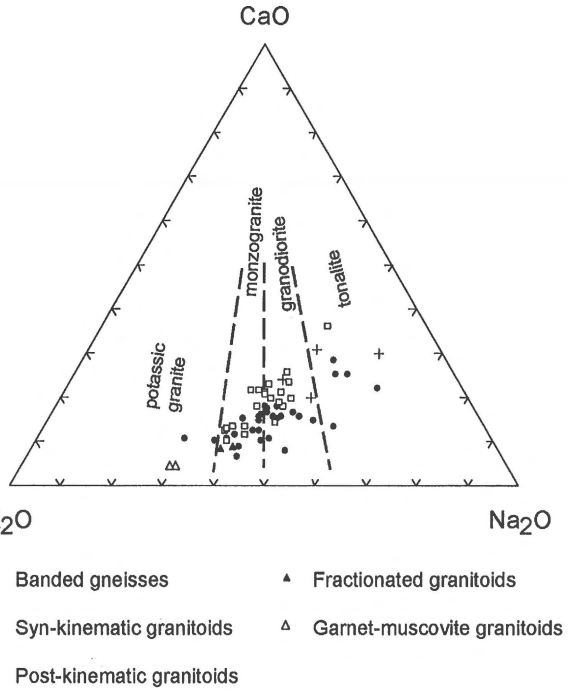

Figure 2. CaO–K_2O–Na_2O plot of granitoids from the Southern Cross region. Analytical data are from the large database of Bettenay (1977). Indicated fields for tonalite, granodiorite, monzogranite and potassic granite according to Condie and Hunter (1976).

preserved cross-cutting relationships show that these veins cut the deformed greenstone, the granitoid as well as the pegmatites.

The adjacent *Lake Deborah Dome* of approximately 1200 km^2 is a half-dome characterised by predominantly subvertical foliations (E–W to N–S strike), made up by elongate feldspar and platy biotite and muscovite crystals, with no evidence of large-scale dynamic recrystallisation. Parallel to this foliation are bands or schlieren of biotite-rich granitoid. The lack of recrystallisation in the minerals which define the foliation and the presence of the schlieren suggest emplacement and deformation of the granitoid in a predominantly magmatic, partially molten state (Paterson et al. 1989). Foliation trajectories in the western half of this dome are concentric. Most foliations dip about verticallly, but locally inward dipping foliations occur (Figure 3A). Only the western contact zone, about 1 km thick and adjacent to the greenstone belt, has tectonic fabrics made up by recrystallised quartz, feldspars and micas, which parallel the greenstone belt. Locally, a secondary, shear-band cleavage suggests dome-up movement. A penetrative mineral lineation occurs in the granitoid in the contact zone with the greenstones, which is defined by elongated, recrystallised quartz and feldspar crystals. Mineral lineations in the greenstone belt west of the dome plunge steeply in a radial pattern, parallel to mineral lineations in the granitoid (Figure 3B). Both the greenstones and the granitoid are intruded by thin pegmatite and aplite dikes which are boudinaged and/or isoclinally folded.

The largest of the domes is the *Ghooli Dome*, which is approximately 80 by 40 km and has an ovoid shape of NNW–SSE orientation. The dome has a broadly concentric foliation which is subhorizontal or gently dipping in its central parts and subvertical along its margins (Figure 3A). These margins are characterised by a 1 to 3-km-wide zone of mylonites and protomylonites. The foliation in this zone is a high-strain tectonic fabric dominated by strong recrystallisation of quartz and feldspars and oriented new growth of muscovite and biotite. This fabric is parallel to the main foliation in the adjacent greenstone belt. Heterogeneous deformation in the central parts of the dome may be deduced from the occurrence of narrow, gently dipping mylonite zones both in gneisses and in relatively weakly deformed granitoid. The foliation throughout the Ghooli Dome is defined by elongated, recrystallised feldspar, quartz and mica. The dome contains widespread greenstone xenoliths, which constitute up to 5% of the outcrops in its central parts. These xenoliths have strong hornblende–plagioclase–biotite foliations which are always parallel to the foliation in the adjacent granitoid.

Mineral and stretching lineations are gently plunging adjacent to the western and northeastern margins of the dome, changing to steep northerly and southerly plunges towards its northern, southern and southeastern edges (Figure 3B). In cases where a secondary, shear-band cleavage occurs in deformed granitoid, its geometry suggests a consistent granitoid-up movement in areas with steeply plunging mineral lineations. To the northeast the dome is cut off abruptly by the Koolyanobbing Shear Zone.

A complex *garnet–muscovite granite* body of irregular shape and relatively minor size occurs about 20 km north of Bullfinch (Figure 1). Measuring some 15 by 5 km, it runs parallel to the general tectonic trend of the greenstone belt. Its host rock consists of greenstone and includes highly deformed rock of mid-amphibolite facies.

A radial pattern of mineral lineations and concentric foliations occurs in the greenstones along the margins. Along the northern margin, foliations gently

dip to the north, and mineral and extension lineations plunge likewise to the north. Along the southern margin, the foliations dip moderately to the south, and the mineral lineations plunge south. Foliation trajectories in the granite are concentric and parallel to the foliation in the bordering greenstones. The intensity of the foliation rapidly decreases towards the centre of the granite. The geometry of a shear-band cleavage (S-C fabric) along the western margin suggests granite-up movement. Although most of the granite–greenstone contacts are concordant, the granite crosscuts the bedding in the greenstone belt on its western margin.

The mineralogy of the granite is characteristic of granites derived from partial melting of metasedimentary rocks (S-type, Chappell & White 1974). The garnet–muscovite granite compositions from Southern Cross plot on the extreme K-rich end (potassic granite) of the Yilgarn granite trend in Figure 2.

The greenstone belt

The Southern Cross greenstone belt is a highly elongate belt of mafic and ultramafic volcanic rocks with a smaller component of banded iron formation (BIF), pelitic rocks and felsic volcanic rocks. Detailed descriptions of the stratigraphy, structure and the metamorphic patterns were presented by Gee (1982) and Ahmat (1986). Deformation and metamorphism are intense, and the degree of structural modification and metamorphism increases towards the margins of the belt.

Four deformation events (D_1–D_4) were recognised in the belt. The first phase, D_1, is characterised by small to large-scale, tight to isoclinal, similar folds. The fold axes plunge subhorizontally NNW–SSE near Southern Cross, and subvertically north of Bullfinch and south of Marvel Loch. First-order D_1 folds of kilometre-scale crop out in the greenstone belt north of Bullfinch and south of Southern Cross (Figures 3A, B). Second-order D_1 folds of a scale of tens of metres crop out at Copperhead, Transvaal and Frasers. Third-order D_1 folds occur throughout the greenstone belt. The axial planes of these folds are in a near-vertical position. A penetrative axial-plane foliation S_1 is associated with D_1. S_1 trends NNW–SSE to N–S in the larger part of the greenstone belt, trends E–W on the southern margin of the Ghooli Dome, and is parallel to the foliation in the margins of the granitoid domes (Figure 3A). S_1 is defined by the alignment of metamorphic amphibole, plagioclase, quartz and ilmenite in amphibolites, by biotite, muscovite and ilmenite in metasedimentary rocks, and by tremolite, chlorite and/or serpentine in metamorphosed ultramafic rocks. The metamorphic amphibole is hornblende on the granitoid–greenstone contacts and actinolite in the centre of the belt.

The second structural event, D_2, is apparent in the major shear zones of the area. These are linear mylonite zones with intense foliation and lineation development along the limbs of D_1 folds, and on granitoid–greenstone contacts. There are at least eight major N–S to NW–SE trending shear zones in the greenstone belts adjacent to the granitoid domes. Two of these have been named: the Koolyanobbing Shear Zone and the Frasers–Corinthia Shear Zone (Figure 3). The fabric in these zones is never folded around the D_1 fold noses, and hence is interpreted as S_2. The Frasers–Corinthia Shear Zone is more than 40 km long and 40 to 150 m wide. Smaller-scale shear zones crop out at Copperhead and Transvaal, and are typically in the order of 5 to 15 m wide. Non-coaxial deformation along these shear zones is inferred from:

i) the displacement of bedding along them;
ii) the presence of shear-band cleavages with discrete angles to the main foliation;
iii) the presence in these zones of asymmetric pressure shadows around clasts, and of rotated porphyroblasts.

The sense of shear is transcurrent in areas with gently plunging mineral lineations (e.g. Frasers–Corinthia Shear Zone), and oblique to dip-slip in areas with steeply plunging mineral lineations (e.g. Copperhead). The orientation of S_2 is subparallel, or slightly oblique to S_1. The S_2 foliation is defined by elongated (actinolitic) hornblende, plagioclase, biotite, chlorite and quartz crystals in amphibolites, by elongated biotite, muscovite, chlorite and quartz in pelitic metasedimentary rocks, and by chlorite, tremolite and talc in ultramafic rocks. Mineral lineations are most clearly developed in amphibolites, where they are defined by parallel elongated hornblende crystals. These mineral lineations are parallel to stretching lineations which are defined by stretched varioles in high-Mg basalts, by stretched pillows in tholeiites, and by stretched pebbles in conglomerates. There are abundant auriferous quartz-sulphide veins with narrow calc-silicate and sulphide alteration haloes in D_2 shear zones (Mueller 1990; Bloem et al. 1994).

The foliation west of the Hamersley Dome is generally subvertical, N to NNW-striking. Subvertical, NNE to NE-striking foliations occur in the northernmost tip of the belt. West of the Lake Deborah Dome, the foliation strikes about NNW with a steep westerly dip. The

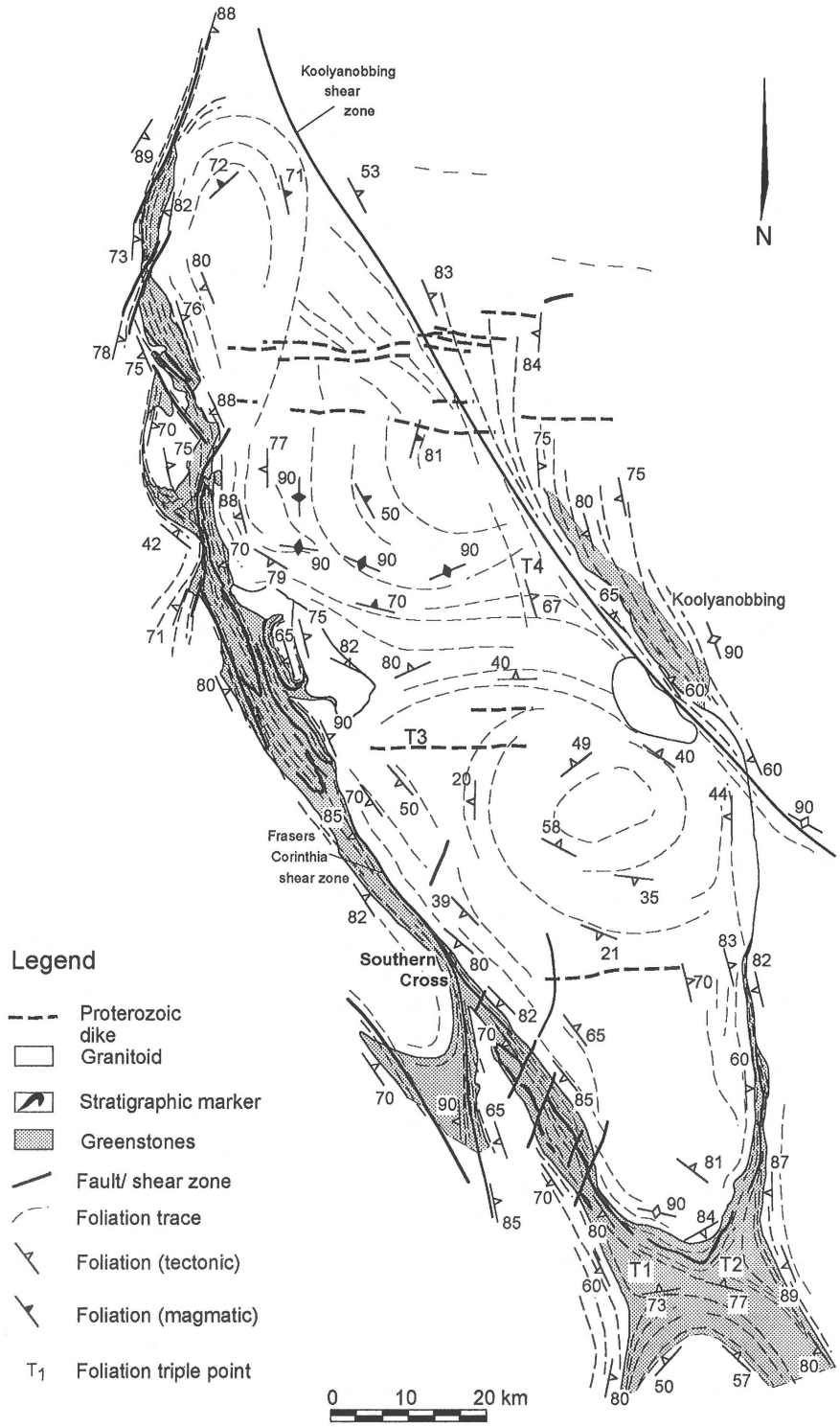

Figure 3A. Regional structural map of the Ghooli Dome complex and the surrounding greenstone belts emphasising folation patterns. The presented foliation traces summarise more than 1300 field measurements of S_1 and S_2. Note the existence of three separate domes within the main batholith, each characterised by concentric foliation patterns.

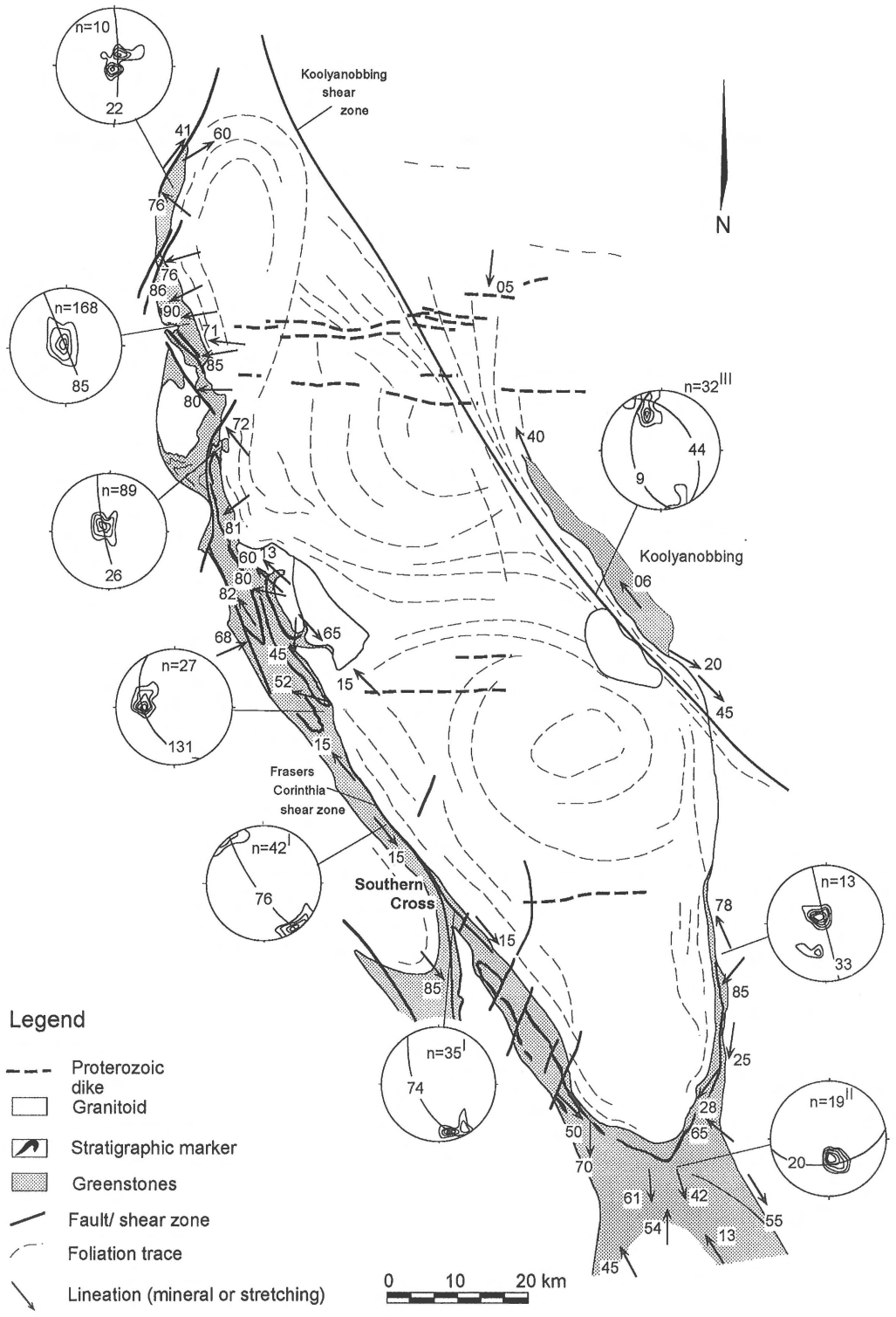

Figure 3B. Regional structural map of the Ghooli Dome complex and the surrounding greenstone belts emphasising mineral lineation patterns (560 measurements). Stereoplots (equal area, lower hemisphere) show the orientations of mineral lineations (contoured, 5% contour interval) and main foliation S_1–S_2 (great circle is the mean orientation, number on great circle is the number of measurements). Additional structural data are from: ^{I} Bloem et al. (1994), ^{II} House (1991), and ^{III} Libby et al. (1991).

same trend dominates west of the Ghooli Dome, but the dip is less, in the order of 50–80° WSW. South of the Ghooli Dome, the folation strikes about east, with a moderate southerly dip. East of the Ghooli Dome, the foliation strikes north, with a subvertical dip. The main foliation in the Koolyanobbing Shear Zone, east of the Ghooli Dome, strikes about NNW with a moderate easterly dip. Locally, there are west-dipping foliations related to localised tight folding of the S_2 foliation around subhorizontal fold axes.

Four foliation triple points occur in the granitoids and the surrounding greenstone belts (Figure 3A). These are located near the northern and southern ends of the Ghooli Dome.

There are moderately NE-plunging lineations in the northernmost tip of the greenstone belt, adjacent to the Hamersley Dome. West of this dome, the lineations plunge steeply W and SW. In the greenstone belt west of the Lake Deborah Dome, the lineations plunge steeply in westerly directions. The plunge of the lineations around the Ghooli Dome is subhorizontal in the area around Southern Cross, and moderate to steep at Bullfinch (50° WNW) and Marvel Loch (70° S). South of the Ghooli Dome, the lineations plunge moderately (40–60° S). East of the Ghooli Dome, the lineations plunge about vertically, although few moderately S-plunging lineations also occur. In the Koolyanobbing Shear Zone, lineations plunge gently to the NNW or SSE. The stereoplots of Figure 3B show the mean greatcircle of the S_1 and S_2 foliations and of mineral- and extension lineations (contoured) for nine subareas in the Southern Cross greenstone belt.

Widespread chocolate-tablet boudinage (i.e. boudinage in which the axes plunge in various directions) of quartz veins and BIF at Southern Cross indicate that the strain here is dominated by flattening (Bloem et al. 1994). In contrast, deformed, cigar-shaped varioles in high-Mg basalts indicate that the deformation near the northern and southeastern ends of the Ghooli Dome, and along the other domes is dominated by subvertical constriction.

The third tectonic pattern, D_3, is characterised by faults which affect the bedding and foliations S_1 and S_2. They indicate that during the deformation the rock properties must have been more brittle than during the previous tectonic phases. NNE-trending D_3 dextral faults offset the Frasers–Corinthia Shear Zone up to 80 m. They also offset the granitoid–greenstone contacts at Bullfinch and south of Southern Cross up to 400 m (Figure 3A). Sinistral, NW-trending faults offset the shear zones up to 20 m. In general the dextral set is more extensively developed. Together, they make up a conjugate set of faults indicative of an ENE–WSW compressional regime. The faults preserve characteristics of ductile deformation such as chlorite fabrics and localised folding, and of brittle deformation such as brittle quartz veins and cataclasites. The S_3 foliation is formed by the preferred orientation of (retrograde) chlorite, carbonate, quartz and graphite in mafic rocks, and is hence distinctively different from the amphibole foliations S_1 and S_2.

The last pattern, D_4, consists of broadly E–W striking, N-dipping, third-order reverse faults developed in the greenstone belt from Southern Cross to Bullfinch and in the Ghooli Dome. The heave to the south on these thrusts is in the order of only a few metres.

Key P-T conditions in plutons and host rock

On the basis of textural criteria in post- and syn-kinematic granitoids, Bettenay (1977) proposed crystallisation pressures in the range of 4 to 5 kbar for most granitoid plutons in the Southern Cross Province. Similar P-T conditions of granitoid emplacement, calculated from amphibole, plagioclase and white-mica mineral chemistry, using three independent geothermobarometers, are summarised in Table 1 and discussed below.

Methodology

Two independent geobarometers were used to determine crystallisation pressures of granitoids. These are the hornblende barometers reviewed by Leake and Said (1994) and the phengite barometer of Velde (1967), later improved by Massonne and Schreyer (1987). The geothermometer of Holland and Blundy (1994) was used to calibrate equilibration temperatures of amphibole–plagioclase pairs in the Ghooli Dome.

Hornblende is a relatively rare phase in granitoids of the Southern Cross Province. Hence, P-T determinations were obtained from small, hornblende-bearing xenoliths in granitoid, under the assumption that they reached thermal equilibrium with the granitoid at the time of crystallisation. These xenoliths have a common mineral assemblage of plagioclase, hornblende, quartz and ilmenite, with or without biotite and epidote. Hornblendes which are in close proximity to the plagioclase, K-feldspar, quartz, biotite, muscovite, magnetite and titanite-bearing granitic wallrock were analysed preferentially. The equilibration temperature

Table 1. Crystallisation pressures and temperatures of granitoids (loc. 1–8) and mineralogy, calculated peak metamorphic pressures and temperatures in greenstones (loc. 9–16) from the Southern Cross region (Figure 1). Ranges in pressure calculations are presented between brackets. Mineral abbreviations: act actinolite, alm almandine, and andalusite, bt biotite, cord cordierite, cpx clinopyroxene, ep epidote, hbl hornblende, ilm ilmenite, Kfsp potassic feldspar, magn magnetite, musc muscovite, oliv olivine, opx orthopyroxene, plag plagioclase, qtz quartz, st staurolite, tnt titanite.

Location	Mineralogy	Reference	P (kbar)	T (°C)
1	plag-Kfsp-qtz-bt-musc-magn-tnt	Massonne & Schreyer, 1987	6.0 ± 1.5* (5.4--6.9)	nd
2	plag-Kfsp-qtz-bt-musc-magn-tnt	Massonne & Schreyer, 1987	5.9 ± 1.5* (5.8--6.0)	nd
3	plag-Kfsp-qtz-bt-musc-magn-tnt	Massonne & Schreyer, 1987	5.3 ± 1.2* (5.1--5.4)	nd
4	plag-Kfsp-qtz-bt-musc-magn-tnt	Massonne & Schreyer, 1987	6.2 ± 1.2* (5.8--6.4)	nd
5	qtz-plag-musc-magn	Massonne & Schreyer, 1987	> 4.6 ± 1.7* (4.0--5.4)	nd
6	plag-hbl-qtz-ilm/magn±tnt±ep±bt	Hammarstrom & Zen, 1986	4.3 ± 1.5* (4.1--4.4)	717 ± 40
7	plag-hbl-qtz-ilm/magn±tnt±ep±bt	Hammarstrom & Zen, 1986	5.9 ± 1.5* (5.8--6.0)	702 ± 40
8	plag-hbl-qtz-ilm/magn±tnt±ep±bt	Hammarstrom & Zen, 1986	5.7 ± 0.8* (5.3--6.2)	732 ± 40
9	bt-musc-alm-plag-and-cord-qtz	Dalstra & Ridley, 1993	3.0 ± 1.5 (2.6--3.1)	560 ± 50
10	and-alm-plag-musc-bt-qtz±st	Dalstra & Ridley, 1993	3.5 ± 1.5 (2.2--4.8)	550 ± 50
11	and-alm-plag-musc-bt-qtz	Bloem et al., 1994	3.7 ± 1.5 (1--6)	520 ± 50
12	and-qtz-musc-ilm	Bohlen et al., 1991	< 4.2 ± 1.8	nd
13	and-cord, and-staur	Mueller, 1990	4.0 ± 1.0 (3--5)	590 ± 40
14	alm-bt-act/hbl-cpx	Mueller, 1990	4.0 ± 1.0 (3--5)	570 ± 50
15	opx-cpx, oliv-opx-qtz	Gole & Klein, 1981	4.0 ± 1.0 (3--5)	670 ± 50
16	bt-musc-cord-qtz±and±alm	McQueen, 1992	3.5 ± 1.0 (3--4)	570 ± 30

* = standard error: standard deviation of the calibrations / √(number of measurements).
nd = not determined.

of amphibole-plagioclase pairs in these xenoliths was calculated additionally with an independent geothermometer to check if thermal equilibrium had indeed been reached between the xenoliths and the surrounding granitoid. This step ensures that variations in the pressure of crystallisation of amphiboles are not merely the result of variations in crystallisation temperature across the pluton. Other complications, such as the ion substitutions in hornblendes, the effects of oxygen fugacity, volatiles and magma compositions have been considered to be negligible for typical granitoid plutons, largely on the basis that similar pressures have been obtained for a range of variables within the same pluton (Leake & Said 1994).

The mineralogical composition of the granitoids at Southern Cross is relatively constant in both granitoid cores and rims. Therefore, no large variations in granitoid crystallisation temperatures across the domes are expected.

The relation between total aluminium content ($Al^T = Al^{IV} + Al^{VI}$) in hornblende and pressure (kbar, Hammarstrom & Zen 1986) is:

$$P = -3.92 + 5.03Al^T$$

Total silica in muscovite depends on pressure, and is discussed by Massonne and Schreyer (1987). This barometer was applied to granitoids containing the assemblage plagioclase, K-feldspar, quartz, biotite, muscovite and magnetite. The presence of the full assemblage ensures that true crystallisation pressures are obtained instead of minimum pressures.

The geothermometer of Holland and Blundy (1994) is based on the thermodynamic evaluation of Al^{IV} in amphibole coexisting with plagioclase in silicate-saturated rocks. The thermometer considers the equilibria: A) edenite + quartz = tremolite + albite, and B) edenite + albite = richterite + anorthite.

Both equilibria yield independent temperatures T^A and T^B of the amphibole–plagioclase equilibration. In this study, T^A and T^B were always within the error margin of 40 °C.

Table 2. Representative microanalyses of amphiboles from the Ghooli granitoid and their application in geobarometry (P) using the calibration of Hammarstrom and Zen (1986) and in geothermometry. The two independent geothermometers T^A and T^B were calculated using Holland and Blundy (1994). Anorthite (Xan) and albite (Xab) contents of coexisting plagioclase crystals are given. See Figure 1 for locations. Amphibole names: MgHbl magnesio hornblende, TschHbl tschermakitic hornblende.

Sample	121431	121431	121431	121431	121495	121495	121495	121497	121497
Location	8	8	8	8	6	6	6	7	7
SiO_2	43.40	43.17	43.56	43.20	44.69	44.76	45.55	42.25	42.94
TiO_2	1.41	1.32	1.39	1.27	1.00	0.85	0.73	0.75	1.33
Al_2O_3	10.99	11.01	10.69	10.87	9.49	9.08	9.61	11.07	10.81
FeO	18.43	18.49	18.61	18.29	17.46	17.37	16.88	22.01	21.86
MnO	0.28	0.32	0.28	0.36	0.26	0.26	0.35	0.25	0.28
MgO	9.85	9.40	9.57	9.38	11.09	10.82	11.39	7.63	7.44
CaO	12.02	11.88	11.93	11.88	12.54	12.33	12.68	12.27	12.13
K_2O	0.92	0.84	0.77	0.91	0.96	0.85	0.91	1.07	1.01
Na_2O	1.12	1.06	1.16	1.11	1.05	0.77	0.84	1.07	1.21
Oxide total	98.42	97.49	97.96	97.27	98.68	97.09	98.94	98.37	99.01
Si	6.42	6.46	6.50	6.49	6.59	6.69	6.66	6.40	6.47
Ti	0.16	0.15	0.15	0.14	0.12	0.10	0.08	0.08	0.15
Al	1.92	1.94	1.88	1.92	1.65	1.60	1.66	1.98	1.92
Fe	2.29	2.31	2.32	2.30	2.15	2.17	2.07	2.79	2.75
Mn	0.04	0.05	0.04	0.05	0.04	0.04	0.04	0.04	0.04
Mg	2.17	2.10	2.12	2.10	2.44	2.41	2.49	1.72	1.67
Ca	1.90	1.91	1.91	1.91	1.98	1.97	1.99	1.99	1.95
K	0.18	0.16	0.14	0.17	0.18	0.16	0.17	0.21	0.19
Na	0.32	0.31	0.33	0.33	0.30	0.22	0.24	0.32	0.35
CatSum	15.40	15.38	15.39	15.42	15.46	15.35	15.39	15.53	15.49
Name	TschHbl	TschHbl	TschHbl	TschHbl	MgHbl	MgHbl	MgHbl	MgHbl	TschHbl
P (kbar) ± 1.5	5.7	5.8	5.5	5.8	4.4	4.1	4.4	6.0	5.7
X(an)	0.37	0.40	0.36	0.39	0.35	0.37	0.36	0.40	0.39
X(ab)	0.63	0.60	0.64	0.61	0.65	0.63	0.64	0.60	0.61
T^A(°C) ± 40	747	736	738	729	757	716	717	764	748
T^B(°C) ± 40	724	718	712	708	710	679	666	708	709

Analytical techniques

A combination of conventional microscopy and electron microscopy was applied to determine stable mineral parageneses and mineral chemistry. Scanning electron microscopy (SEM) at the Centre for Microscopy and Microanalysis (CMM) of the University of Western Australia (UWA) was used to discriminate possible cryptic zonations in minerals, and to determine mineral compositions. Microanalyses for the major elements in silicates from selected samples were performed on a JEOL JSM 6400 using a LINK EDS X-ray analysis system, a normally incident beam, a take-off angle of 40°, and a counting time of 60 s. The accelerating voltage was 15 kV at a beam current of 3.0 nA. In-house software (RECALC 2) was used to recalculate mineral formulae from the raw oxide data, and to calibrate Fe^{3+} on the basis of ideal mineral stoichiometry.

Results of geothermometry and geobarometry

The amphiboles are euhedral, dark-green tschermakitic hornblendes or magnesio-hornblendes with relatively low silica contents and moderate to high titanium contents. Representative amphibole analyses are presented in Table 2, together with the anorthite contents (ranging from 35–40%) of coexisting plagioclase crystals and the calculated temperatures of equilibra-

Table 3. Representative microanalyses of white micas from the Ghooli granitoid, and their application in geobarometry using the calibration of Massonne and Schreyer (1987). See Figure 1 for locations.

Sample	121501	121501	121501	121502	121502	121502	121503	121503	121503	121504	121504	121504	121505	121505	121505
Location	1	1	1	2	2	2	3	3	3	4	4	4	5	5	5
SiO_2	44.99	44.41	45.75	45.52	45.75	45.93	45.57	45.75	44.79	46.06	45.30	45.22	45.50	45.72	45.01
Al_2O_3	30.39	29.81	31.05	32.20	31.97	32.39	32.94	32.96	32.13	32.34	31.10	32.46	34.78	33.89	34.83
Cr_2O_3	0.00	0.00	0.00	0.00	0.00	0.00	0.00	0.00	0.00	0.00	0.00	0.00	0.00	0.00	0.00
FeO	5.45	5.79	4.08	4.22	4.33	4.36	4.32	3.93	4.14	3.33	4.52	3.20	2.13	2.45	2.44
MgO	1.77	1.82	0.89	0.43	0.45	0.32	0.49	0.39	0.30	0.42	0.65	0.42	0.22	0.38	0.15
Na_2O	0.00	0.00	0.00	0.18	0.22	0.00	0.20	0.23	0.16	0.18	0.00	0.22	0.16	0.00	0.28
K_2O	11.17	11.23	11.28	11.33	11.58	11.41	11.01	11.15	11.11	11.20	11.22	11.09	11.22	11.26	11.10
Oxide total	94.05	93.65	93.42	94.08	94.67	94.80	94.92	95.05	93.15	94.00	93.38	93.11	94.20	93.98	93.81
Si	3.12	3.11	3.17	3.13	3.14	3.14	3.10	3.11	3.11	3.15	3.15	3.13	3.09	3.11	3.07
Al	2.49	2.46	2.53	2.61	2.58	2.61	2.64	2.64	2.63	2.61	2.55	2.64	2.78	2.72	2.80
Cr	0.00	0.00	0.00	0.00	0.00	0.00	0.00	0.00	0.00	0.00	0.00	0.00	0.00	0.00	0.00
Fe^{2+}	0.32	0.34	0.24	0.24	0.25	0.25	0.25	0.22	0.24	0.19	0.26	0.19	0.12	0.14	0.14
Mg	0.18	0.19	0.09	0.04	0.05	0.03	0.05	0.04	0.03	0.04	0.07	0.04	0.02	0.04	0.02
Na	0.00	0.00	0.00	0.02	0.03	0.00	0.03	0.03	0.02	0.02	0.00	0.03	0.02	0.00	0.04
K	0.99	1.00	1.00	1.00	1.01	0.99	0.96	0.97	0.99	0.98	0.99	0.98	0.97	0.98	0.97
CatSum	7.11	7.13	7.04	7.06	7.07	7.04	7.05	7.04	7.05	7.02	7.05	7.03	7.01	7.00	7.03
P(kbar) ± 3.0	5.6	5.4	6.9	5.8	6.0	6.0	5.1	5.4	5.4	6.4	6.4	5.8	>4.5	>5.4	>4.0

tion (Holland & Blundy 1994). The temperature of equilibration is about 720 ± 40 °C at the three locations which were sampled in this study, which about equals the estimated temperature of crystallisation of a granodiorite or monzogranite pluton (e.g. Bettenay 1977). This suggests that the xenoliths in the dome were heated to granitoid crystallisation temperatures during pluton emplacement. The corresponding average pressures of hornblende crystallisation using the calibration of Hammarstrom and Zen (1986) are 4.3 to 5.9 kbar (Table 1).

Representative muscovite analyses are presented in Table 3. The analysed muscovites are euhedral to subhedral and colourless. They have relatively low silica, high potassium, and moderate iron contents. The calculation of the pressure of crystallisation is graphical. The average pressures of crystallisation of white micas in granitoid from the Ghooli Dome, using the entire dataset, is 4.6 to 6.2 kbar. Crystallisation pressures derived from the Massonne and Schreyer (1987) barometer are incorporated in Table 1.

The crystallisation pressures and temperatures for all locations shown in Figure 1 are summarised in Table 1. Crystallisation pressures were in the order of 4.3 to 5.9 kbar in the centre, and were 5.3 to 6.2 kbar along the margins of the Ghooli Dome. The standard errors, defined as: the standard deviation of the techniques (3 kbar), divided by the square root of the number of measurements on individual minerals, are 0.8 to 1.7 kbar. Although the differences are just within the error margin of most barometric calibrations, the trend is from higher crystallisation pressures at the granitoid–greenstone contact to lower pressures in the core of the granitoid dome.

In the greenstone belts, P-T conditions at the peak of metamorphism were determined from critical mineral assemblages and a set of geothermobarometers (Gole & Klein 1981, Mueller 1990, McQueen 1992, Dalstra & Ridley 1993, Bloem et al. 1994). Peak metamorphic pressures in the greenstone belts are 1 to 2 kbar lower than crystallisation pressures in the granitoid domes, and there is a trend towards lower pressures in the cores of the belts. For example, andalusite is the only stable Al-silicate phase in the greenstone belt north of Nevoria, and thus metamorphic pressures there were below 4.2 kbar (Bohlen et al. 1991). Metamorphic pressures in the Southern Cross area were in the order of 3.0 to 3.7 (± 1.5) kbar at temperatures of 520 to 560 °C (Dalstra & Ridle 1993, Bloem et al. 1994). Along the greenstone-belt margins at Marvel Loch, Nevoria and Mt Palmer, P-T conditions were 4.0 (± 1.0) kbar at temperatures of 570 to 670 °C (Gole & Klein 1981, Mueller 1990, McQueen 1992). The highest peak metamorphic temperature (670 °C) is recorded from the narrowest section of the greenstone belt at Mt Palmer.

Large poikiloblasts of unstrained cordierite, andalusite, garnet and staurolite with straight inclusion trails, which are parallel to the foliation in the rock, overgrow the S_1 fabric of quartz, biotite, mus-

covite and ilmenite outside the D_2 shear zones. Within these zones, porphyroblasts are flattened, have rotated inclusion trails and pressure shadows, and the mylonitic foliation wraps around them. Thus, metamorphic prophyroblasts grew syn-kinematically in D_2 shear zones, but generally post-kinematically outside them. This suggests that peak metamorphic conditions in the greenstone belts were reached during and shortly after regional D_1 deformation and were broadly synchronous with D_2. Retrograde conditions (chlorite, carbonate, graphite) existed during D_3 with the formation of brittle fault zones.

The available pressure data from the Southern Cross greenstone belt suggest maximum burial depths in the order of 10 to 13 km, approximately 4 to 7 km less than the crystallisation depths of the bordering granitoids, assuming that the calibrated pressures reflect burial depth only.

Age of the Ghooli granitoid

Sampling and analytical techniques

A large sample from the central Ghooli Dome was collected for radiometric dating of the granitoid. The sample site is approximately 20 km NNE of Bullfinch (Figure 1, Location 8). It consists of approximately 15 by 5 km of semi-continuous outcrop and is the largest uniform granitoid outcrop in the dome. The magmatic foliation, defined by elongate feldspar clasts and biotite schlieren, is concordant to the regional concentric foliation pattern in the dome, suggesting that, at this location, the granitoids form a coherent part of the dome.

The granitoid at the sample site is a massive, coarse-grained, biotite-bearing monzonite. The magmatic foliation, which is defined by biotite schlieren, strikes NW to W. The granitoid is cross-cut by medium-grained, equigranular biotite-granite dikes, and by younger aplite dikes.

Zircons were separated from the granitoid sample (UWA no. 121509) and analysed with a Sensitive High Resolution Ion Microprobe (SHRIMP II) using established methods (Compston et al. 1984, Williams et al. 1984) and the CZ3 zircon standard (564 Ma). Uncertainties in ages are quoted at the 95% confidence level.

Results

The sample yielded abundant, mostly small crystals. The zircons are subhedral to euhedral, and generally very short. The smallest, mostly clear zircons are generally subhedral. Some larger zircons are rounded. Most zircons are unzoned, except for some, partly metamict, crystals which show concentric zoning patterns. These also have darker cores with more intense zonation.

Raw, ^{204}Pb-corrected data are summarised in Table 4. Fifteen zircon analyses were calibrated against eight standards with a calibration error of 1.93%. Three zircon analyses were processed against two standards with a calibration error of 6.23%. The $^{207}Pb/^{206}Pb$ ages do not show a consistent trend from cores to rims. All analyses plot in a tight cluster on the concordia diagram, suggesting a single zircon population with an age of 2691 ± 7 Ma (Figures 4A, B). Figure 5 shows a $^{207}Pb/^{206}Pb$ versus $^{204}Pb/^{206}Pb$ plot of the same zircons. The data plot in a tight cluster close to the $^{207}Pb/^{206}Pb$ axis, representing low contents of common lead. Four analyses, however, define a linear trend which represents mixing between zircon lead and lead from the surrounding rock.

Processing the data in separate groups, and omitting the data which are less than 95% concordant and the analyses which were calibrated against the less accurate standard analyses, does not significantly change the result (the $^{207}Pb/^{206}Pb$ age for nine analyses which are more than 95% concordant is 2694 ± 9 Ma). Therefore, the weighted mean $^{207}Pb/^{206}Pb$ age of 2691 ± 7 Ma of the concordant to near-concordant analyses is considered to be the crystallisation age of the granitoid.

Discussion

Interpretation of the structural events

In summary, the diagnostic structural features in the Southern Cross belt are: i) flow folding forming large to small-scale upright folds and a penetrative axial-plane foliation (S_1) during D_1, ii) mylonitisation and foliation reorientation during D_2, iii) transcurrent faulting with minor foliation reorientation during D_3, and iv) reverse faulting during D_4. D_1 to D_3 represent progressive, ductile and later brittle–ductile deformation in a broadly ENE–WSW compressional regime. D_4 is possibly a simple relaxation of the E–W compressional regime which prevailed during D_1–D_3. Peak metamor-

Table 4. SHRIMP II analytical data (^{204}Pb corrected) and errors (+/- is 1 σ) for zircons from location 8 (Ghooli Dome; sample UWA 121509). 4f^{206}Pb is a measure of the fraction of ^{206}Pb derived from common lead. %conc is the degree of concordancy of the analysis. Age is calculated in millions of years.

Zircon no.	core/ rim	U/ppm	Th/ppm	4f^{206}Pb	^{207}Pb/^{206}Pb	+/-	^{208}Pb/^{206}Pb	+/-	^{206}Pb/^{238}U	+/-	^{207}Pb/^{235}U	+/-	%conc	Age ^{207}Pb/^{206}Pb	+/-
F1-1	rim	367	387	0.005238	0.1833	0.0010	0.2908	0.0022	0.478	0.010	12.07	0.26	94	2682	9
E1-1	core	356	455	0.007937	0.1816	0.0012	0.3704	0.0028	0.447	0.009	11.18	0.24	89	2667	11
E2-1	core	162	201	0.004953	0.1868	0.0015	0.3397	0.0034	0.491	0.010	12.64	0.29	95	2714	13
C2-1	rim	373	532	0.033316	0.1837	0.0024	0.4820	0.0057	0.349	0.007	8.83	0.22	72	2686	22
A3-1	rim	92	99	0.010468	0.1802	0.0025	0.2628	0.0055	0.473	0.010	11.76	0.32	94	2655	23
B3-1	rim	464	313	0.001218	0.1848	0.0007	0.1843	0.0012	0.496	0.010	12.62	0.26	96	2696	6
C3-1	rim	201	136	0.001854	0.1847	0.0012	0.1852	0.0024	0.503	0.010	12.81	0.29	97	2696	11
D3-1	core	234	251	0.001559	0.1840	0.0010	0.2882	0.0023	0.502	0.010	12.72	0.28	97	2689	9
A3-2	rim	109	107	0.013668	0.1895	0.0029	0.2772	0.0064	0.415	0.009	10.84	0.30	82	2738	25
A4-1	core	79	74	0.007308	0.1832	0.0024	0.2618	0.0052	0.499	0.011	12.61	0.35	97	2682	22
D1-1	core	170	222	0.031563	0.1864	0.0035	0.3388	0.0079	0.315	0.007	8.10	0.24	65	2710	31
D4-1	core	66	61	0.012158	0.1832	0.0032	0.2427	0.0068	0.504	0.012	12.74	0.39	98	2682	29
F4-1	core	277	264	0.008849	0.1841	0.0016	0.2844	0.0036	0.510	0.011	12.94	0.30	99	2690	15
E6-1	core	88	83	0.004338	0.1861	0.0025	0.2616	0.0054	0.572	0.014	14.69	0.43	108	2708	22
F4-2	rim	317	300	0.010168	0.1832	0.0018	0.2735	0.0040	0.497	0.031	12.56	0.81	97	2682	16
A6-1	core	156	131	0.010316	0.1811	0.0030	0.2432	0.0065	0.526	0.033	13.13	0.89	102	2663	27
B6-1	core	441	582	0.006586	0.1850	0.0014	0.3484	0.0033	0.562	0.035	14.33	0.92	107	2699	13
C6-1	rim	381	518	0.001459	0.1845	0.0013	0.3798	0.0031	0.556	0.035	14.15	0.91	106	2694	11

phic conditions were broadly synchronous with D_1 and D_2, which is indicated by the growth parallel to both S_1 and S_2 of hornblende in amphibolites and of biotite, muscovite and cordierite in metapelitic rocks. Retrograde conditions existed during D_3, as indicated by the growth of chlorite and siderite parallel to S_3 in D_3 fault zones only.

The granitoid domes at Southern Cross were probably emplaced syntectonically during the regional structural event D_1–D_2 because:

i) they have elongated, ovoid outlines perpendicular to the inferred D_1–D_2 compression direction;

ii) the main foliations S_1 and S_2 are concordant across the granitoid–greenstone contacts, and are strongest at the contacts;

iii) metamorphic minerals (syn-D_1 and D_2) indicate mid-amphibolite facies conditions at the contacts and upper-greenschist facies within the centre of the belt. In other words, the domes have contact-metamorphic haloes in which the peak-metamorphic minerals grew synchronously with D_1 and D_2. Also, the presence of deformed, syntectonic pegmatitic and aplitic veins in the host rocks, and xenoliths in the contact zones suggests high P-T conditions during emplacement;

iv) D_3 fault zones transect and offset the granitoid–greenstone contacts, which suggests pre-D_3 emplacement of the plutons.

The formation of the regional D_1 foliation must have postdated crystallisation of the Ghooli granitoid at 2691 Ma, because this foliation occurs in, and is always parallel in, granitoids, greenstones and xenoliths of greenstone in granitoids. The absolute timing of the second, shear-zone-forming event D_2 is constrained by the 2636–2620 Ma age of the gold deposits within these shear zones (McNaughton et al. 1990, Bloem et al. 1995, Qiu et al. in press). The D_3 and D_4 events took place under retrograde conditions after 2620 Ma.

Gently dipping foliations in the centre, and the abundance of greenstone xenoliths in the contact zone suggest that the present erosion level cuts relatively close to the roof of the Ghooli Dome. In the Lake Deborah and Hamersley Domes the present erosion level cuts deeper. This can be deduced from the occurrence of steep and locally inward dipping magmatic fabrics and an absence of greenstone xenoliths in the central parts of these domes. Steep, locally inward dipping foliations in granitoid domes are a diagnostic feature of the lower levels of diapirs (Van den Eeckhout et al. 1986; Figure 1).

Tectonic concepts

Three contrasting structural concepts can potentially account for the present map pattern of granitoids and greenstone belts in the Southern Cross Province of the Yilgarn Block. These are discussed below:

1) *Regional dome and basin folding* of a granitic basement covered by a greenstone sequence with an

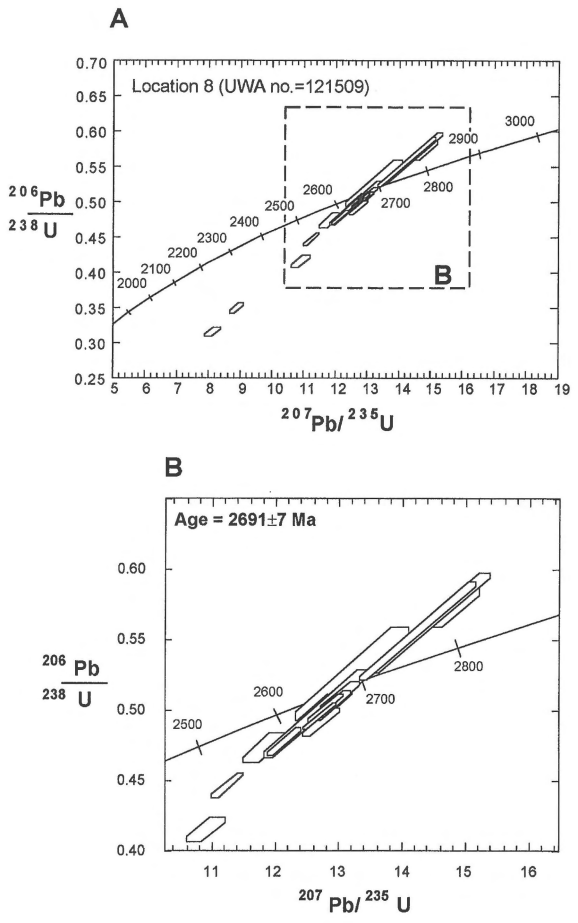

Figure 4. A) $^{206}Pb/^{238}U$ versus $^{207}Pb/^{235}U$ (concordia) plot of zircons from sample UWA 121509 from location 8 (Ghooli Dome). Error boxes are 1 σ. *B)* Enlargement of *A)*, showing concordant to near-concordant analyses.

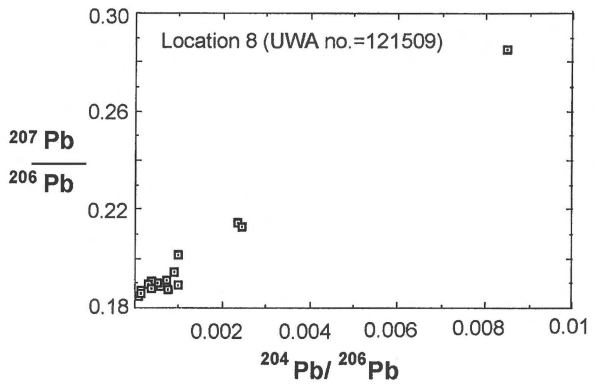

Figure 5. $^{207}Pb/^{206}Pb$ versus $^{204}Pb/^{206}Pb$ plot of zircons from sample UWA 121509 from location 8 (Ghooli Dome).

older subhorizontal structural grain, or folding of a granitic substrate (e.g. Ahmat 1986).

2) *Regional extension*, producing structures similar to metamorphic core complexes in which the granitoids and high-grade greenstone margins represent the metamorphic cores (e.g. Williams & Whitaker 1993).
3) *Regional diapirism*, involving uprise of granitoids in older greenstones. The most important diagnostic criteria for a diapir are the rise of the core material relative to its overburden, and the rise of the central part of the structure relative to its outer margins (Bateman 1984, Van den Eeckhout et al. 1986).

Both the dome and basin-folding and metamorphic core-complex concepts predict the dominance of older ages in the cores of the granitoid domes because basement reactivation in both tectonic regimes is limited. The available geochronological data, however, suggest younger crystallisation ages for the granitic rocks than for the greenstone cover, which was dated at 3000–3020 ± 50 Ma (Bickle et al. 1983, Fletcher et al. 1984). Moreover, lineation patterns around most of the domes are radial, or tangential radial, which is incompatible with a dome and basin-folding or core-complex concept. Finally, there is no direct evidence, such as mutually perpendicular foliations within the granitoid domes, for a regional dome and basin-folding event.

The diapiric rise of the granitoids relative to their country rocks at Southern Cross is indicated by consistent granitoid-up movement senses on shear zones along the granitoid–greenstone contacts. Calculated pressures of crystallisation of the Ghooli Dome granitoid that are higher than calculated peak-metamorphic pressures in adjacent greenstone belts also suggest rise of the granitoid relative to greenstones after crystallisation of the former. In addition, the granitoid–greenstone terrain at Southern Cross shows a number of features which are highly suggestive of diapiric emplacement (e.g. Dixon & Summers 1983, Ridley 1989):

i) ovoid diapir outlines and closed circular trends of the foliations near the contact. Linear foliation trends are clearly related to later structures such as the Koolyanobbing Shear Zone;
ii) conformable structures across the intrusive contact in both the diapir and the covering greenstones;
iii) radial or tangential–radial (stretching) lineation patterns in the greenstones. The smaller-scale granitoid domes are characterised by radial lineation patterns, whereas the Ghooli Dome shares a com-

bination of radial and tangential lineation patterns in its country rocks;

iv) strain in the greenstone belt is dominated by strong horizontal contraction with planes of flattening subparallel to the granitoid–greenstone interface at Southern Cross. Towards the foliation triple points (Nevoria, Bullfinch, Figure 3A) vertical constrictive strain dominates, as is indicated by subvertical mineral and stretching lineations;

v) peak metamorphic temperatures in the greenstone belt are reached during or shortly after regional (D_1–D_2) deformation, and metamorphic mineral assemblages are synkinematic to postkinematic with respect to these deformation phases;

vi) tensional shear zones with aplite and pegmatite intrusions and quartz–sulphide veins and gold mineralisation are most abundant in the country rocks adjacent to the Ghooli Dome. The present erosion level is close to the roof of this dome, and hence structures in the dome and its country rocks are likely to be dilational. These veins may thus have formed from high-pressure fluid intrusions from the diapiric core into the country rock.

The relatively high pressure of crystallisation throughout the granitoids, relative to the peak metamorphic pressures in the adjacent greenstone belts, suggests that the granitoids rose up to 6 km relative to the greenstones, as partly consolidated blocks, to depths of 10 to 13 km, after initial emplacement at crustal levels of 14 to 20 km. During this uplift, most of the strain was concentrated on the granitoid–greenstone contacts, on which mylonites developed locally.

The elongate shape of the diapirs is consistent with the presence of a regional E-W to ENE–WSW compressional regime which prevailed during the diapiric rise of the plutons. The complex foliation and lineation patterns in the Southern Cross Province reflect the intricacy of the stress patterns during the granitoid emplacement.

Diapirism can thus explain many of the observed regional structural patterns in the Southern Cross area, and a diapiric model for this terrain seems to be appropriate.

Gold mineralisation

The Southern Cross greenstone belt is host to at least six lode-gold occurrences with total pre-mining resources of more than 10 tons of gold each. Five of these major occurrences are in greenstones adjacent to the Ghooli Dome in close proximity to the granitoid–greenstone contact (Copperhead, Frasers, Marvel Loch, Mt Palmer and Nevoria, Figure 1). A number of smaller occurrences (Marie's Find, Corinthia, Transvaal and several others) are also close to that dome. The largest deposits (Copperhead, Marvel Loch, Mt Palmer and Nevoria) are located towards the northern and southern ends of the dome, close to foliation triple points.

A time relationship between regional deformation, dome emplacement and gold mineralisation in the Copperhead, Corinthia, Frasers, Marvel Loch, Maries Find and Nevoria deposits can be argued as follows:

i) the gold occurrences are structurally controlled in D_2 shears, and spatially related to the Ghooli Dome;

ii) ore shoots are offset by D_3 faults, which also offset the granitoid–greenstone contacts;

iii) ore-shoots and mineral and extension lineations in country rocks plunge parallel (Figure 6);

iv) the orientation of gold-bearing structures varies with respect to their position relative to the granitoid dome;

v) alteration assemblages, ore assemblages and textures in all the gold occurrences suggest that mineralisation occurred under elevated P-T conditions which were similar or slightly retrograde to peak metamorphic conditions in the lower to mid-amphibolite facies (Mueller 1990, Barnicoat et al. 1991, Dalstra & Ridley 1993; Bloem et al. 1994). The gold occurs in quartz vein arrays and as an integral part of the high-temperature wallrock alteration around these veins, suggesting a hydrothermal origin for gold mineralisation in all deposits.

Bloem et al. (1995) demonstrated that gold mineralisation at the Corinthia deposit occurred just prior to 2620 Ma, and hence was broadly synchronous with other gold occurrences in the Yilgarn Block (McNaughton et al. 1990; Qiu et al. in press). Such a time constraint potentially poses problems for a direct link between the granitoids and the gold mineralisation and its hosting structures, since age determinations of syn-kinematic granitoids in the Yilgarn Block suggest that the major period of emplacement was from 2691 to 2660 Ma (Hill et al. 1992). The only known felsic intrusive event which broadly coincides with gold mineralisation is the intrusion of syn-kinematic charnockitic granitoids at 2627 (± 12) Ma in high-grade gneiss terrain, approximately 150 km SW of Southern Cross (Wilde & Pidgeon 1987; Qiu et al. in press). The emplacement of these granitoids was broadly synchronous with regional metamorphism and with the gold

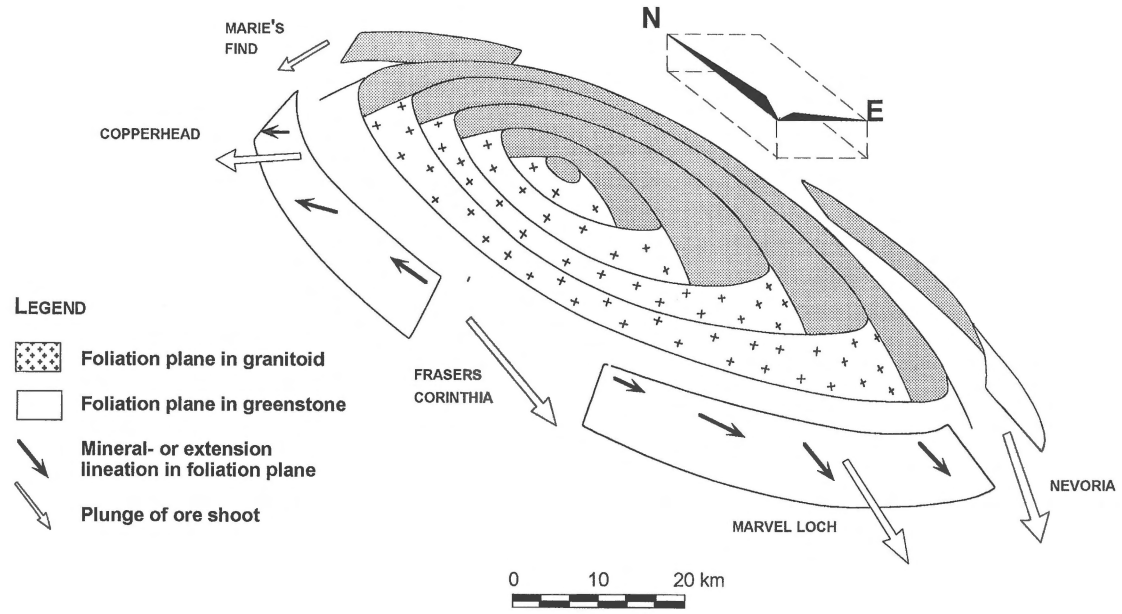

Figure 6. Schematic structural model for the Ghooli Dome and for the gold mineralisation in the greenstone belt. Shown are the orientations of mineral lineations in the greenstone belt and the plunge directions of ore shoots in deposits discussed in the text.

mineralisation at Griffins Find at 2636 ± 3 Ma (Wilde & Pidgeon 1987; Barnicoat et al. 1991).

Despite the sparsity of high-precision geochronological data, the following tectonic scenario for the Southern Cross region is proposed:

1) Deposition of greenstone-belt rock sequences on a felsic basement at about 3000 Ma;

2) Widespread melting of this felsic basement and recrystallisation of these melts, resulting in granitoid crystallisation at about 2691–2660 Ma, at depths of approximately 19 km. From that time onwards, the sequence remained hot, until:

3) Regional ENE–WSW compression started diapiric rise of the granitoids to depths of 10 to 13 km from 2636 to 2620 Ma. The granitoids deformed their margins and the bordering greenstones, and expelled large amounts of overpressured fluids in the overlying strata. Channeling of these fluids into shear zones, and interaction of the fluids with rocks favourable for gold precipitation were the major causes for formation of the gold deposits in the Southern Cross belt;

4) Cooling and deformation under retrogressive conditions.

Conclusions

1) In the Southern Cross region, concentric foliation and lineation patterns in the large granitoid domes and in their surrounding wall rocks strongly suggest the diapiric emplacement of the granitoids after their initial crystallisation at depth. The diapiric rise coincided wit the first two (D1 and 2) of four tectonic phases (D1–4) recognised in the field.
2) Crystallisation of the large granitoid domes at Southern Cross most likely occurred between 2691 and 2660 Ma.
3) Crystallisation pressures in the core of the dome are slightly lower than those on the dome margin. This suggests that the crystallisation of the core took place at a shallower depth than the crystallisation of the margins, and hence, the pluton was already rising during the process of crystallisation.
4) The crystallisation pressure of the Ghooli Dome, in the order of 4.3 to 6.2 kbar, is about 2 kbar higher than peak-metamorphic pressures in the greenstone belt (about 3.0–4.0 kbar). This suggests that the granitoid rose 5 to 6 km after crystallisation, relative to the greenstone belt.
5) Diapirism in a regional tectonic regime of E–W to ENE–WSW compression, from 2636 to 2620 Ma, is the most plausible concept for pluton emplace-

ment. Among the alternatives considered, this best reconciles the calculated P-T data, the observed structural patterns, and the timing, location and orientation of the mineral-bearing structures.

6) The large gold occurrences in the central Southern Cross Province are spatially related to the Ghooli Dome. The important gold deposits formed in the pressure shadow zones of this dome, implying a correlation between mineralisation, diapiric granitoid rise and E–W compression synchronous with the tectonic phases D_1 and D_2 at 2636 to 2620 Ma.

Acknowledgements

Special thanks go to Marion Dahl and Neal McNaughton for their assistance with the radiometric dating. HJD and EJMB are recipients of Overseas Postgraduate Research Scholarships and University of Western Australia Research Scholarships. HJD is recipient of an Australian Geological Survey Organisation Scholarship. This research project was also supported by the Schürmann Foundation (The Hague, Netherlands), grant no. 1994/13. Zircon analyses were carried out on a Sensitive High Resolution Ion Microprobe (SHRIMP II) operated by a consortium consisting of Curtin University of Technology, The Geological Survey of Western Australia and the University of Western Australia with the support of the Australian Research Council.

References

Ahmat, A.L. 1986 Metamorphic patterns in the greenstone belts of the Southern Cross Province, Western Australia – Geol. Survey West. Aust. Prof. Paper 19: 1–21

Archibald, N.J., L.F. Bettenay, M.J. Bickle & D.I. Groves 1981 Evolution of Archaean crust in the Eastern Goldfields Province of the Yilgarn Block, Western Australia – Spec. Publ. Geol. Soc. Aust. 7: 491–504

Barnicoat, A.C., R.J. Fare, D.I. Groves & N.J. McNaughton 1991 Syn-metamorphic lode-gold deposits in high-grade Archean settings – Geology 19: 921–924

Bateman, R.J. 1984 On the role of diapirism in the segregation, ascent and final emplacement of granitoid magmas – Tectonophysics 110: 211–231

Bettenay, L.F. 1977 Regional geology and petrogenesis of Archean granitoids in the southeastern Yilgarn Block, Western Australia – Unpublished PhD Thesis, Univ. of Western Australia, Nedlands, W.A., 238 pp

Bickle, M.J., H.J. Chapman, L.F. Bettenay & D.I. Groves 1983 Lead ages, reset rubidium-strontium ages and implications for the Archaean crustal evolution of the Diemals area, Central Yilgarn Block, Western Australia – Geochim. Cosmochim. Acta 47: 907–914

Bloem, E.J.M., H.J. Dalstra, D.I. Groves & J.R. Ridley 1994 Metamorphic and structural setting of amphibolite-hosted gold deposits between Southern Cross and Bullfinch, Southern Cross Province, Yilgarn Block, Western Australia – Ore Geol. Reviews 9: 183–208

Bloem, E.J.M., N.J. McNaughton, D.I. Groves & J.R. Ridley 1995 An indirect lead isotope age determination of gold mineralisation at the Corinthia Mine, Yilgarn Block, Western Australia – Aust. J. Earth Sci. 42: 447–451

Bohlen, S.R., A. Montana & D.M. Kerrick 1991 Precise determinations of the equilibria kyanite = sillimanite and kyanite = andalusite and a revised triple point for the Al_2SiO_5 polymorphs – Am. Mineral. 76: 677–680

Chappell, B.W. & A.J.R. White 1974 Two contrasting granite types – Pacific Geol. 8: 173–174

Compston, W., I.S. Williams & C. Myer 1984 U-Pb geochronology of zircons from Breccia 73217 using a sensitive high mass-resolution ion microprobe – Proc. 14th Lunar Sci. Conf. J. Geophys. Suppl. 89: 525–534

Condie, K.C. & D.R. Hunter 1976 Trace element geochemistry of Archaean granitic rocks from the Barberton region, South Africa – Earth Planet. Sci. Lett. 29: 389–400

Dalstra, H.J. & J.R. Ridley 1993 Gold mineralisation in contrasting metamorphic terrains: Evidence for heterogeneous deformation and diachronous metamorphism, Southern Cross Province, Western Australia. In: P.F. Hach, A.J. Torres, F. Gervilla & R. Gervilla (eds.): Current Research in Geology Applied to Ore Deposits. Granada, Spain: 437–440

Dixon, J.M. & J.M. Summers 1983 Patterns of total and incremental strain in subsiding troughs: experimental centrifuged models of inter-diapir synclines – Can. J. Earth Sci. 20: 1843–1861

Feng, R. & R. Kerrich 1992 Geodynamic evolution of the Southern Abitibi and Pontiac terranes: evidence from geochemistry of granitoid magma series (2700–2630 Ma) – Can. J. Earth Sci. 29: 2266–2286

Fletcher, I.R., K.J.R. Rosman, I.R. Williams, A.F. Hickman & J.L. Baxter 1984 Sm-Nd geochronology of greenstone belts in the Yilgarn Block, Western Australia – Precambrian Res. 26: 333–361

Gee, R.D. 1982 Southern Cross, Western Australia – 1 : 250000 Geological Series – Geol. Survey West. Aust. Explanatory Notes

Gole, M.J. & C. Klein 1981 High-grade metamorphic Archaean banded iron formations, Western Australia: assemblages with coexisting pyroxenes ± fayalite – Am. Mineral. 66: 87–99

Groves, D.I. 1993 The crustal continuum model for late-Archaean lode-gold deposits of the Yilgarn Block, Western Australia – Mineralium Deposita 28: 366–374

Hammarstrom, J.M. & E. Zen 1986 Aluminium in hornblende: An empirical igneous geobarometer – Am. Mineral. 71: 1297–1313

Hill, R.I., B.W. Chappell & I.H. Campbell 1992 Late Archaean granites of the southeastern Yilgarn Block, Western Australia: age, geochemistry and origin – Trans. Roy. Soc. Edinburgh: Earth Sci. 83: 211–226

Holland, T.J.B. & J.D. Blundy 1994 Non-ideal interactions in calcic amphiboles and their bearing on amphibole-plagioclase geothermometry – Contrib. Mineral. Petrol. 116: 433–447

House, M. 1991 Structural and geophysical studies of the Banker Saddle area, Southern Cross greenstone belt, Western Australia – Unpublished BSc (Hons) Thesis, Univ. of Western Australia, Nedlands, W.A., 62 pp

Leake, B.E. & Y.A. Said 1994 Hornblende barometry of the Galway batholith, Ireland: an empirical test – Mineral. Petrol. 51: 243–250

Libby, J., D.I. Groves & J.R. Vearncombe, 1991 The nature and tectonic significance of the crustal-scale Koolyanobbing shear zone, Yilgarn Craton, Western Australia – Aust. J. Earth Sci. 38: 229–245

Massonne, H.J. & W. Schreyer 1987 Phengite geobarometry based on the limiting assemblage with K-feldspar, phlogopite, and quartz – Contrib. Mineral. Petrol. 96: 212–224

McNaughton, N.J., K.F. Cassidy, D.I. Groves & C.S. Perring 1990 Timing of mineralization. In: S.E. Ho, D.I. Groves & J.M. Bennet (eds.): Gold Deposits of the Archaean Yilgarn Block, Western Australia: Nature, Genesis and Exploration Guides. Geol. Dept. (Key Centre) & Univ. Extension, Univ. West. Australia, Publ. 20: 221–226

McQueen, K.G. 1992 The Great Victoria gold deposit, Marvel Loch, Western Australia: Retrograde gold mobilization in a metamorphosed sulphidic iron formation. In: J.E. Glover & S.E. Ho (eds.): The Archaean: Terrains, Processes and Metallogeny. Geol. Dept. (Key Centre) & Univ. Extension, Univ. West. Australia, Publ. 22: 365–380

Mueller, A.G. 1990 The nature and genesis of high- and medium-temperature Archaean gold deposits in the Yilgarn Block, Western Australia, including a specific study of scheelite-bearing gold skarn deposits – Unpublished PhD Thesis, Univ. of Western Australia, Nedlands, W.A., 144 pp

Paterson, S.R., R.H. Vernon & O.T. Tobisch 1989 A review of the criteria for the identification of magmatic and tectonic foliations in granitoids – J. Struct. Geol. 11(3): 349–363

Qiu, J., N.J. McNaughton, D.I. Groves & H.J. Dalstra (in press) SHRIMP U-Pb in zircon and lead isotope constraints on the timing and source of an Archaean granulite hosted lode-gold deposit at Griffins Find, Yilgarn Block, Western Australia – Special Issue of Chronique de la Recherche Minière

Ridley, J.R. 1989 Vertical movement in orogenic belts and the timing of metamorphism relative to deformation. In: J.S. Daly, R.A. Cliff & B.W.D. Yardley (eds.): Evolution of Metamorphic Belts. Geol. Soc. Spec. Publ. 43: 103–115

Van den Eeckhout, B., J. Grocott & R. Vissers 1986 On the role of diapirism in the segregation, ascent and final emplacement of granitoid magmas – discussion – Tectonophysics 127: 161–169

Velde, B. 1967 Si^{+4} content of natural phengites – Contrib. Mineral. Petrol. 14: 250–258

Wilde, S.A. & R.T. Pidgeon 1987 U-Pb geochronology, geothermometry and petrology of the main areas of gold mineralization in the Wheat Belt region of Western Australia – West. Aust. Mining Petrol. Res. Inst. Rept. 30, 171 pp

Williams, I.S., W. Compston, L.P. Black, T.R. Ireland & J.J. Foster 1984 Unsupported radiogenic Pb in zircon: a cause of anomalously high Pb-Pb, U-Pb and Th-Pb ages – Contrib. Mineral. Petrol. 88: 322–327

Williams, P.R. & A.J. Whitaker 1993 Gneiss domes and extensional deformation in the highly mineralised Archaean Eastern Goldfields Province, Western Australia – Ore Geol. Reviews 8: 1–22